

## Isospin mixing in nuclei around $N \simeq Z$ and the superallowed $\beta$ -decay\*

W. SATUŁA<sup>1,2</sup>, J. DOBACZEWSKI<sup>1,3</sup>, W. NAZAREWICZ<sup>4,5,1</sup>,  
AND M. RAFALSKI<sup>1</sup>

<sup>1</sup>Institute of Theoretical Physics, University of Warsaw, ul. Hoża 69,  
PL-00-681 Warsaw, Poland

<sup>2</sup> KTH (Royal Institute of Technology), AlbaNova University Center,  
106 91 Stockholm, Sweden

<sup>3</sup>Department of Physics, University of Jyväskylä, P.O. Box 35 (YFL),  
FI-40014 Finland

<sup>4</sup>Department of Physics & Astronomy, University of Tennessee,  
Knoxville, Tennessee 37996, USA

<sup>5</sup>Physics Division, Oak Ridge National Laboratory, P.O. Box 2008,  
Oak Ridge, Tennessee 37831, USA

Theoretical approaches that use one-body densities as dynamical variables, such as Hartree-Fock or the density functional theory (DFT), break isospin symmetry both explicitly, by virtue of charge-dependent interactions, and spontaneously. To restore the spontaneously broken isospin symmetry, we implemented the isospin-projection scheme on top of the Skyrme-DFT approach. This development allows for consistent treatment of isospin mixing in both ground and excited nuclear states. In this study, we apply this method to evaluate the isospin impurities in ground states of even-even and odd-odd  $N \simeq Z$  nuclei. By including simultaneous isospin and angular-momentum projection, we compute the isospin-breaking corrections to the  $0^+ \rightarrow 0^+$  superallowed  $\beta$ -decay.

PACS numbers: 21.10.Hw, 21.60.Jz, 21.30.Fe, 23.40.Hc

---

\* Presented at the International Conference on Nuclear Structure *Nuclear Landscape at the Limits*, Zakopane, Poland, 2010.

## 1. Introduction

The atomic nucleus is a quantum system composed of the two types of strongly interacting fermions, the nucleons. The charge independence of the nuclear interaction is at the roots of the isospin symmetry [1, 2]. This concept remains valid even in the presence of Coulomb interaction, which is the major source of the isospin breaking. This is so because of the smallness of the isospin-breaking isovector and isotensor components of the Coulomb field as compared to the isospin-conserving components of the nuclear and Coulomb forces.

The isotopic spin quantum number,  $T$ , provides strong selection rules for nuclear reactions, decays, and transitions [3]. In particular, the selection rules for  $\beta$ -decay Fermi and Gamow-Teller transitions are  $\Delta T = 0$  and  $\Delta T = 0, \pm 1$ , respectively, with the exception of  $T = 0 \rightarrow T = 0$  transitions that are forbidden [4, 5]. The superallowed  $0^+ \rightarrow 0^+$  Fermi transitions bridge nuclear structure with the electroweak standard model of particle physics, providing the most accurate estimate for the  $V_{ud}$  matrix element of the CKM matrix [6, 7]; hence, testing the CKM unitarity. From a nuclear structure perspective, the unitarity test depends critically on a set of theoretically calculated isospin-breaking corrections whose precise determination poses a challenging problem [8, 9, 10].

In this work, we calculate the isospin impurities and isospin-breaking corrections to the superallowed Fermi decay by using a newly developed isospin- and angular-momentum-projected DFT approach without pairing [11, 12, 13]. This technique takes advantage of the ability of the mean field (MF) to properly describe long-range polarization effects. The MF treatment is followed by the isospin projection to remove the unwanted spontaneous isospin mixing within MF [12, 14, 15, 16].

This paper is organized as follows. We begin in Sec. 2 with a short summary of our isospin- and angular-momentum-projected DFT approach. In Sec. 3, we present applications of the isospin-projected DFT variant of the model to the isospin mixing in the ground states (g.s.) of even-even  $N=Z$  nuclei. Section 4 discusses preliminary results for the isospin-breaking corrections to the superallowed beta decays calculated by considering simultaneous isospin and angular-momentum restoration. Finally, the conclusions are contained in Sec. 5.

## 2. Theory

The isospin-projected DFT technique [11, 12, 13] utilizes the ability of the self-consistent MF method to properly describe the balance between the long-range Coulomb force and the short-range nuclear interaction, represented in this work by the Skyrme-type energy density functional (EDF).

To remove the spurious isospin-symmetry-breaking effects, we use the standard one-dimensional isospin projection after variation, which allows us to decompose the Slater determinant  $|\Phi\rangle$  into good isospin states  $|T, T_z\rangle$ :

$$|\Phi\rangle = \sum_{T \geq |T_z|} b_{T, T_z} |T, T_z\rangle, \quad \sum_{T \geq |T_z|} |b_{T, T_z}|^2 = 1. \quad (1)$$

Here,  $\hat{P}_{T_z T_z}^T$  stands for the conventional one-dimensional isospin-projection operator:

$$\begin{aligned} |TT_z\rangle &= \frac{1}{\sqrt{N_{TT_z}}} \hat{P}_{T_z T_z}^T |\Phi\rangle \\ &= \frac{2T+1}{2\sqrt{N_{TT_z}}} \int_0^\pi d\beta_T \sin \beta_T d_{T_z T_z}^T(\beta_T) \hat{R}(\beta_T) |\Phi\rangle, \end{aligned} \quad (2)$$

where  $\beta_T$  denotes the Euler angle associated with the rotation operator  $\hat{R}(\beta_T) = e^{-i\beta_T \hat{T}_y}$  about the  $y$ -axis in the isospace,  $d_{T_z T_z}^T(\beta_T)$  is the Wigner function [17], and  $T_z = (N - Z)/2$  is the third component of the total isospin  $T$ . The normalization factors  $N_{TT_z}$ , or interchangeably the expansion coefficients  $b_{T, T_z}$  that encode the isospin content of  $|\Phi\rangle$ , read:

$$\begin{aligned} N_{TT_z} &\equiv |b_{T, T_z}|^2 = \langle \Phi | \hat{P}_{T_z T_z}^T | \Phi \rangle \\ &= \frac{2T+1}{2} \int_0^\pi d\beta_T \sin \beta_T d_{T_z T_z}^T(\beta_T) \mathcal{N}(\beta_T), \end{aligned} \quad (3)$$

where  $\mathcal{N}(\beta_T) = \langle \Phi | \hat{R}(\beta_T) | \Phi \rangle$  is the so-called overlap kernel. For technical aspects concerning the calculation of the overlap and Hamiltonian kernels, we refer the reader to Ref. [13]. The isospin-projected DFT technique utilizes the ability of the HF solver HFODD [18] to produce fully symmetry-unrestricted Slater determinants  $|\Phi\rangle$ .

The isospin projection determines the set of good isospin states (called the *basis* in the following), which in the next step is used to rediagonalize the entire nuclear Hamiltonian, consisting of the kinetic energy, Skyrme EDF, and the isospin-breaking Coulomb force. The rediagonalization leads to the eigenstates:

$$|n, T_z\rangle = \sum_{T \geq |T_z|} a_{T, T_z}^n |T, T_z\rangle, \quad (4)$$

numbered by index  $n$ . The amplitudes  $a_{T, T_z}^n$  define the degree of isospin mixing through the so-called isospin-mixing coefficients (or isospin impurities) for the  $n$ -th eigenstate:

$$\alpha_C^n = 1 - |a_{T, T_z}^n|_{\max}^2, \quad (5)$$

where  $|a_{T,T_z}^n|_{\max}^2$  stands for the squared norm of the dominant amplitude in the wave function  $|n, T_z\rangle$ . It is worth stressing that the isospin projection, unlike particle-number or angular-momentum projections, is essentially non-singular; hence, it can be safely used with the local EDFs. The rigorous analytical proof of this useful property can be found in Ref. [13].

The combined isospin and angular-momentum projection leads to the set of states,

$$|I, M, K; T, T_z\rangle = \frac{1}{\sqrt{N_{TT_z;IMK}}} \hat{P}_{T_z T_z}^T \hat{P}_{MK}^I |\Phi\rangle, \quad (6)$$

which form another normalized basis built on  $|\Phi\rangle$ . Here,  $\hat{P}_{T_z T_z}^T$  and  $\hat{P}_{MK}^I$  stand for the isospin and angular-momentum projection operators, respectively, and  $M$  and  $K$  denote the angular-momentum components along the laboratory and intrinsic  $z$ -axes, respectively [19]. Now the problem becomes more complicated because of the overcompleteness of the basis (6) related to the  $K$ -mixing. This is overcome by performing the re-diagonalization of the Hamiltonian in the so-called *collective space*, spanned for each  $I$  and  $T$  by the *natural states*,  $|IM; TT_z\rangle^{(i)}$ , as described in Refs. [18, 20]. Such a re-diagonalization gives the solutions:

$$|n; IM; T_z\rangle = \sum_{i, T \geq |T_z|} a_{iIT}^{(n)} |IM; TT_z\rangle^{(i)}, \quad (7)$$

which are labeled by the index  $n$  and by the conserved quantum numbers  $I$ ,  $M$ , and  $T_z = (N - Z)/2$  [cf. Eq. (4)].

### 3. Isospin mixing

By using the perturbation theory [22] and the analytically solvable hydrodynamical model [23], the isospin mixing in atomic nuclei has been studied since the 1960s (see Ref. [24] for a review). These simple approaches accounted for such qualitative features of the isospin impurities like the steady increase in  $N = Z$  nuclei with increasing proton number and strong quenching with increasing  $|N - Z|$ . Quantitatively, however, their predictions for the values of the isospin impurities  $\alpha_C$  were not very reliable.

Increased demand for accurate values of isospin mixing has been stimulated by the recent high-precision measurements of superallowed  $\beta$ -decay rates [6, 7]. Large-scale shell-model approaches [25], although very accurate in the description of configuration mixing, can hardly account for the long-range polarization exerted on the neutron and proton states by the Coulomb force whose accurate treatment requires using large configuration spaces. In contrast, in self-consistent DFT, such polarization effects are

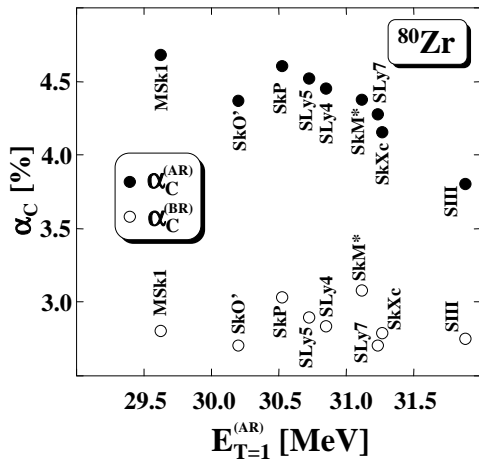


Fig. 1. Isospin impurities in the ground state of  $^{80}\text{Zr}$ , predicted by DFT, using various Skyrme parametrizations [21] plotted versus the corresponding excitation energies of the  $T = 1$  doorway states. Open dots mark results obtained before the Coulomb rediagonalization (BR),  $\alpha_C^{(BR)} = 1 - |b_{T=[T_z, T_z]}|^2$ , which were calculated by using expansion coefficients of Eq. (1). Full dots mark the impurities (5) obtained after the Coulomb rediagonalization (AR).

naturally accounted for by finding the proper balance between the Coulomb force, which tends to make the proton and neutron states different, and the isoscalar part of the strong force, which has an opposite tendency.

In general, isospin impurities determined without removing spurious isospin mixing are underestimated by about 30% compared to the values obtained after rediagonalization [12]. In the particular case of  $^{80}\text{Zr}$ , the removal of spurious admixtures increases  $\alpha_C$  from  $\sim 2.9\%$  to  $\sim 4.4\%$ , as illustrated in Fig. 1. It is encouraging to see that the latter value agrees well with the central value of empirical impurity deduced from the giant dipole resonance  $\gamma$ -decay studies, as communicated during this meeting by F. Camera *et al.* [26]. Unfortunately, experimental error bars are too large to discriminate between various Skyrme parametrizations, which differ in predicted values of  $\alpha_C$  by as much as  $\sim 10\%$ .

Figure 2 illustrates our attempts to correlate the values of  $\alpha_C$  with the surface and volume symmetry energies, which are primary quantities characterizing the isovector parts of nuclear EDFs. The linear regression coefficients shown in the figure hardly indicate any correlation of  $\alpha_C$  with these quantities. In fact, no clear correlation was found between the calculated values of  $\alpha_C$  and other bulk characteristics of the Skyrme EDFs, including the isovector and isoscalar effective masses, and incompressibility.

#### 4. Isospin-breaking corrections to the Fermi matrix elements of the superallowed $\beta$ -decay

An accurate evaluation of  $\alpha_C$  is a prerequisite for determining the isospin-breaking correction  $\delta_C$  to the  $0^+ \rightarrow 0^+$  Fermi matrix element of the

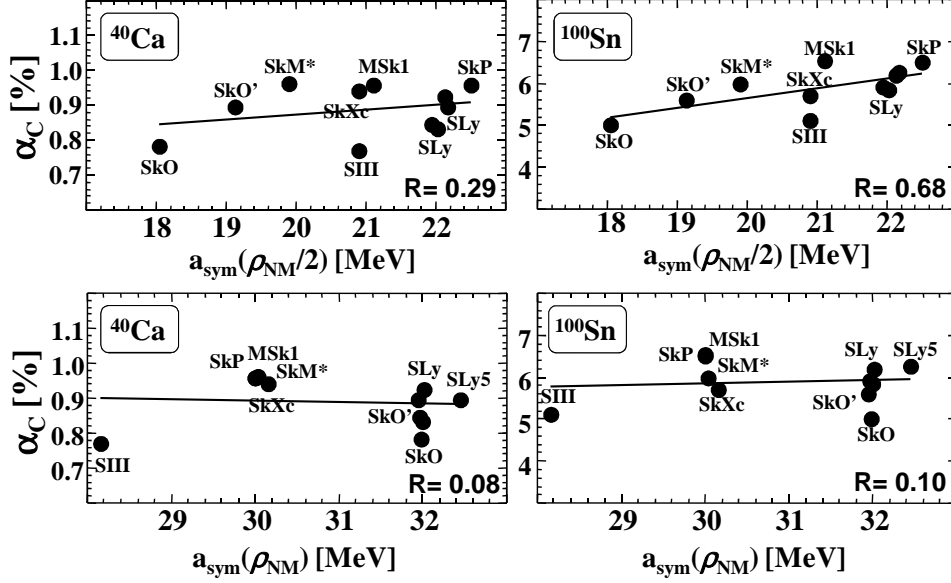


Fig. 2. Isospin impurities predicted by several Skyrme EDFs for the ground states of  $^{40}\text{Ca}$  (left) and  $^{100}\text{Sn}$  (right) plotted versus the surface (top) and volume (bottom) symmetry energy.

isospin raising/lowering operator  $\hat{T}_{\pm}$  between nuclear states connected by the superallowed  $\beta$ -decay:

$$|\langle I^{\pi} = 0^{+}, T \approx 1, T_z = \pm 1 | \hat{T}_{\pm} | I^{\pi} = 0^{+}, T \approx 1, T_z = 0 \rangle|^2 \equiv 2(1 - \delta_C). \quad (8)$$

Here, the state  $|I^{\pi} = 0^{+}, T \approx 1, T_z = \pm 1\rangle$  corresponds to the g.s. of the even-even nucleus whereas  $|I^{\pi} = 0^{+}, T \approx 1, T_z = 0\rangle$  denotes its isospin-analogue in the neighboring  $N = Z$  odd-odd nucleus. Unlike the former one, the odd-odd configuration cannot be expressed in a form of a MF product wave function [13]. Therefore, to compute the states in odd-odd  $N = Z$  nuclei, we use the following strategy (see Fig. 1 of Ref. [13] for a schematic illustration):

- Firstly, we compute the so-called antialigned g.s. configuration,  $|\bar{\nu} \otimes \pi\rangle$  or  $|\nu \otimes \bar{\pi}\rangle$ , by placing the odd neutron and the odd proton in the lowest available time-reversed (or signature-reversed) single-particle Nilsson orbits.
- Secondly, to correct for the fact that the antialigned configurations manifestly break the isospin symmetry, that is,  $|\bar{\nu} \otimes \pi\rangle \approx \frac{1}{\sqrt{2}}(|T = 0\rangle +$

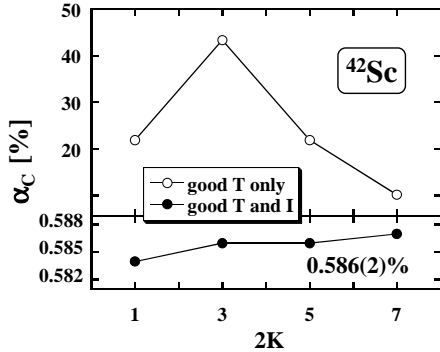


Fig. 3. Isospin impurities in  $^{42}\text{Sc}$ , calculated for four antialigned configurations that are obtained by putting the valence neutron and proton in opposite- $K$  Nilsson orbitals originating from the  $f_{7/2}$  shell, that is,  $|\nu\bar{K} \otimes \pi K\rangle$  with  $K = 1/2, 3/2, 5/2$ , and  $7/2$ . Open and full dots show the results obtained by employing only the isospin projection and simultaneous isospin and angular-momentum ( $I = 0$ ) projection, respectively.

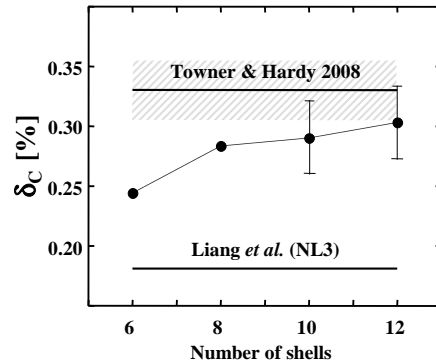


Fig. 4. Isospin-breaking correction to the Fermi matrix element for the super-allowed transition  $^{14}\text{O} \rightarrow ^{14}\text{N}$ . Full dots represent our results plotted as a function of the basis size (number of HO shells taken in HF calculations). A conservative 10% error was assigned to the last two points. The values quoted in Refs. [7] (including errors) and [27] are shown for comparison.

$|T = 1\rangle$ ), we apply the simultaneous isospin and angular-momentum projection to create the good isospin and good angular momentum basis  $|I, M, K, T, T_z = 0\rangle$  of Eq. (6).

- Finally, to obtain the state  $|I = 0, T \approx 1, T_z = 0\rangle$ , we re-diagonalize the total Hamiltonian, including the Coulomb term, in the new basis [cf. Eq. (7)].

The projected  $|I^\pi = 0^+, T \approx 1, T_z = \pm 1\rangle$  states in even-even nuclei are computed in the same way.

Restoration of angular momentum turns out to be the key ingredient in evaluation of the isospin impurity in odd-odd nuclei. This is illustrated in Fig. 3, which shows  $\alpha_C$  calculated for the  $T \approx 1$  states in  $^{42}\text{Sc}$ . Four solutions shown in Fig. 3 correspond to the four possible antialigned MF configurations built on the Nilsson orbits originating from the spherical  $\nu f_{7/2}$  and  $\pi f_{7/2}$  subshells. These configurations can be labeled in terms of the  $K$  quantum numbers,  $K = 1/2, 3/2, 5/2$ , and  $7/2$ , as  $|\nu\bar{K} \otimes \pi K\rangle$ . In a simple shell-model picture, each of those MF states contains all  $I=0$ ,

2, 4, and 6 components. From the results shown in Fig. 3, it is evident that the isospin projection alone (upper panel) leads to unphysically large impurities, whereas the impurities obtained after the isospin and angular-momentum ( $I=0$ ) projection (lower panel with the scale expanded by the factor of 500) are essentially independent of the initial MF configuration, as expected. The average value and standard deviation of 0.586(2)% shown in the figure were obtained for the configuration space of  $N = 10$  spherical harmonic oscillator (HO) shells, whereas for  $N = 12$  the analogous result is 0.620(2)% (see below).

Although indispensable, the angular-momentum projection creates numerous practical difficulties when applied in the context of DFT, that is, with energy functional rather than Hamiltonian. The major problem is the presence of singularities in energy kernels [28]. Although appropriate regularization schemes have already been proposed [29], they have neither been tested nor implemented. This fact narrows the applicability of the model only to those EDF parametrizations which strictly correspond to an interaction, wherefore the singularities do not appear. For Skyrme-type functionals, this leaves only one EDF parametrization, namely SV [30]. This specific EDF contains no density dependence and, after including all tensor terms in both time-even and time-odd channels, it can be related to a two-body interaction. Despite the fact that for basic observables and characteristics such as binding energies, level densities, and symmetry energy, SV performs poorly, we have decided to use it in our systematic calculations of  $\delta_C$ . Indeed, while SV would not be our first choice for nuclear structure predictions, it is still expected to capture essential polarization effects due to the self-consistent balance between the long-range Coulomb and short-range nuclear forces.

In order to test the performance of our model, we have selected the superallowed  $\beta$ -decay transition  $^{14}\text{O} \rightarrow ^{14}\text{N}$ . This case is particularly simple, because (i) the participating nuclei are spherical and almost doubly magic, which implies suppressed pairing correlations, and (ii) the antialigned configuration in  $^{14}\text{N}$  involves a single  $|\nu\bar{p}_{1/2} \otimes \pi p_{1/2}\rangle$  configuration that is uniquely defined. The predicted values of  $\delta_C$  are shown in Fig. 4 as a function of the assumed configuration space (that is, the number of spherical HO shells  $N$  used). While the full convergence has not yet been achieved, this result, taken together with other tests performed for heavier nuclei, suggests that at least  $N = 10$  shells are needed for light nuclei ( $A < 40$ ), whereas at least  $N = 12$  shells are required for heavier nuclei. The resulting systematic error due to basis cut-off is estimated at the level of  $\sim 10\%$ .

Even though calculations for all heavy ( $A > 40$ ) nuclei of interest are yet to be completed, and due to the shape-coexistence effects there are still some ambiguities concerning the choice of global minima, our very prelim-

inary results are encouraging. Namely, the mean value of the structure-independent statistical-rate function  $\bar{\mathcal{F}}t$ , obtained for 12 out of 13 transitions known empirically with high precision (excluding  $^{38}\text{K} \rightarrow ^{38}\text{Ar}$  case), equals  $\bar{\mathcal{F}}t = 3069.4(10)$ , which gives the  $V_{\text{ud}} = 0.97463(24)$  amplitude of the CKM matrix. These values match very well those obtained by Towner and Hardy in their latest compilation [7]. That said, owing to the poor quality of the SV parameterization, the confidence level [10] of our results is low. On a positive note, our method is quantum mechanically consistent (see discussion in Ref. [8]) and contains no free parameters.

## 5. Summary

In summary, the isospin- and angular-momentum-projected DFT theory has been employed to calculate isospin mixing and isospin-breaking corrections to the  $0^+ \rightarrow 0^+$  Fermi superallowed  $\beta$ -decay. Our parameter-free model capitalizes on the ability of the MF approach to describe long-range polarization effects. The self-consistent HF wave functions containing essential correlations due to the symmetry-breaking mechanism are then used as trial states during the projection procedure. The results for  $\alpha_C$  in  $^{80}\text{Zr}$  are consistent with current experimental estimates from the giant dipole resonance studies. The preliminary results on the  $\delta_C$ -corrections are also very encouraging. The calculated values of the nucleus-independent  $\bar{\mathcal{F}}t = 3069.4(10)$  and the  $V_{\text{ud}} = 0.97463(24)$  are consistent with the recent evaluations of Ref. [7].

This work was supported in part by the Polish Ministry of Science under Contracts numbers N N202 328234 and N N202 239037, Academy of Finland and University of Jyväskylä within the FIDIPRO programme, and by the Office of Nuclear Physics, U.S. Department of Energy under Contract Nos. DE-FG02-96ER40963 (University of Tennessee) and DE-FC02-09ER41583 (UNEDF SciDAC Collaboration). We acknowledge the CSC - IT Center for Science Ltd, Finland for the allocation of computational resources.

## REFERENCES

- [1] W. Heisenberg, Z. Phys. **77**, 1 (1932).
- [2] E.P. Wigner, Phys. Rev. **51**, 106 (1937).
- [3] *Isospin in nuclear physics*, ed. D.H. Wilkinson (North Holland, Amsterdam, 1969).
- [4] E.P. Wigner, Phys. Rev. **56**, 519 (1939).
- [5] H. Daniel and H. Schmitt, Nucl. Phys. **65**, 481 (1965).

- [6] J.C. Hardy and I.S. Towner, Phys. Rev. C **71**, 055501 (2005); Phys. Rev. Lett. **94**, 092502 (2005); Phys. Rev. C **79**, 055502 (2009).
- [7] I.S. Towner and J.C. Hardy, Phys. Rev. C **77**, 025501 (2008).
- [8] G.A. Miller and A. Schwenk, Phys. Rev. C **78**, 035501 (2008).
- [9] G.A. Miller and A. Schwenk, Phys. Rev. C **80**, 064319 (2009).
- [10] I.S. Towner and J.C. Hardy, arXiv:1007.5343.
- [11] M. Rafalski, W. Satuła, and J. Dobaczewski, Int. J. Mod. Phys. **E18**, 958 (2009).
- [12] W. Satuła, J. Dobaczewski, W. Nazarewicz, and M. Rafalski, Phys. Rev. Lett. **103**, 012502 (2009).
- [13] W. Satuła, J. Dobaczewski, W. Nazarewicz, and M. Rafalski, Phys. Rev. C **81**, 054310 (2010).
- [14] C.A. Engelbrecht and R.H. Lemmer, Phys. Rev. Lett. **24**, 607 (1970).
- [15] E. Caurier, A. Poves, and A. Zucker, Phys. Lett. B **96**, 11 (1980); **96**, 15 (1980).
- [16] E. Caurier and A. Poves, Nucl. Phys. **A385**, 407 (1982).
- [17] D.A. Varshalovich, A.N. Moskalev, and V.K. Khersonskii, *Quantum Theory of Angular Momentum* (World Scientific, Singapore, 1988).
- [18] J. Dobaczewski, W. Satuła, B.G. Carlsson, J. Engel, P. Olbratowski, P. Powalowski, M. Sadziak, J. Sarich, N. Schunck, A. Staszczak, M.V. Stoitsov, M. Zalewski, and H. Zduńczuk, Comput. Phys. Commun. **180**, 2361 (2009).
- [19] P. Ring and P. Schuck, *The Nuclear Many-Body Problem* (Springer-Verlag, Berlin, 1980).
- [20] H. Zduńczuk, W. Satuła, J. Dobaczewski, and M. Kosmulski, Phys. Rev. C **76**, 044304 (2007).
- [21] M. Bender, P.-H. Heenen, and P.-G. Reinhard, Rev. Mod. Phys. **75**, 121 (2003).
- [22] L.A. Sliv and Yu.I. Kharitonov, Phys. Lett. **16**, 176 (1965).
- [23] A. Bohr, J. Damgård, and B. Mottelson, in *Nuclear Structure*, ed. by A. Hossian *et al.* (North-Holland Publ. Co., Amsterdam, 1967).
- [24] N. Auerbach, Phys. Rep. **98**, 273 (1983).
- [25] W.E. Ormand and B.A. Brown, Phys. Rev. C **52**, 2455 (1995).
- [26] F. Camera *et al.*, *these proceedings*.
- [27] H. Liang, N. Van Giai, and J. Meng, Phys. Rev. C **79**, 064316 (2009).
- [28] H. Zduńczuk, J. Dobaczewski, and W. Satuła, Int. J. Mod. Phys. E **16**, 377 (2007).
- [29] D. Lacroix, T. Duguet, and M. Bender, Phys. Rev. C **79**, 044318 (2009).
- [30] M. Beiner, H. Flocard, N. Van Giai, and P. Quentin, Nucl. Phys. **A238**, 29 (1975).